BISMUTH BASED NANO-COMPOSITES& THEIR POTENTIAL APPLICATIONS AS PHOTOCATALYST: A CRITICAL REVIEW ON WASTE WATER TREATMENT

Hafiz Talha Akhtar[1*], Muhammad Irslan Ilyas[1], Toseef Fatima[1,] Nazia Parveen[2], Muhammad Alyas Habib[2], Hassan Nawaz[3], Muhammad Usman Amin[3], Muhammad Ayaz Ashraf [3]

Faculty of Sciences, Department of Chemistry, The University of Lahore

Faculty of Sciences, International Islamic University Islamabad

University of management and technology Lahore

ABSTRACT

Bismuth (Bi) is a versatile metal widely utilized in various fields, particularly in catalysis. It forms composites with different metals, serving as efficient photocatalysts. These bismuth-based composites are crafted through innovative methods like sol-gel, microwave, and co-precipitation using nanotechnology. They exhibit remarkable photocatalytic prowess, degrading organic substances and detecting heavy metals through UV, sunlight, and visible light irradiation. Notable heavy metals such as Pb, arsenic, titanium, Cr, and Ni, along with organic pollutants like MB, CO, AO, NP, malonic acid, and diphenylhydrazine, have been detected using these composites. Bismuth's transitional nature contributes to its promising photocatalytic abilities. A comprehensive review spanning 1963 to 2019 highlights bismuth's exceptional efficacy as a photocatalyst for wastewater treatment. Bi-TNT (bismuth-titanate nanotube) composites, synthesized via one-step or two-step anodization methods, Demonstrate increased photocatalytic performance in treating industrial wastewater using visible light. The composites are analyzed using techniques including FE-SEM, EDS, XRD, UV-Vis DRS, and XPS for characterization purposes. Their improved photodegradation results are attributed to bismuth deposition.

INTRODUCTION

Photocatalysis employs visible-light-responsive catalysts (e.g., TiO2, ZnO, ZnS, CdS, BiVO4, g-C3N4) for eco-friendly pollutant removal and solar-driven energy production, including diverse semiconductors (metal selenides, phosphides, halides)[1]. Bismuth, a metalloid, adopts a rhombohedral lattice with a two-atom unit cell structure[2]. Bismuth, initially mistaken for lead and tin, was differentiated by Claude François Geoffroy in 1753 and later utilized in an 1860s London Stock Exchange scam falsely promising its conversion into silver[3]. Bismuth's relative crustal abundance is 0.008 ppm. It's found in ores like bismuthinite, bismite, and in native form, being non-toxic and non-carcinogenic[4]. Bismuth's band structure was determined from multiple experiments, with their limited influence on outcomes expected[5]. Nanoscale's transformative nanostructures, bridging atomic and bulk scales via high surface-to-volume ratio, drive diverse applications through manipulation and novel attributes[6]. "Nano," rooted in Latin and Greek for "dwarf," represents 10^{-9} scale, driving transformative nanotechnology with unique materials impacting diverse fields[6]. Nanotechnology involves the exploration and advancement of substances, structures, and apparatuses at the scale of molecules or atoms, often centered on matter around 100 nm in size[7]. Nanotechnology produces novel nanomaterials with distinct properties via atom-level manipulation, applicable across electronics, energy, healthcare, and more, driven by high surface-to-volume ratio and quantum phenomena[8]. Nanotechnology revolutionizes the food industry by enhancing packaging, shelf life, impurity detection, and additive integration while preserving taste neutrality[9]. Nanotechnology in medicine utilizes nanoparticles for disease detection/treatment, including drug/gene therapy, cancer treatment, MRI contrast, tissue regeneration, and pathogen identification[10]. Nanotechnology enables small, fast, high-storage, low-power devices like smart cards, digital cameras, liquid crystals, LEDs, and

nano-transistors[11]. Nanotechnology improves renewable energy by utilizing nanomaterials for increased efficiency, corrosion resistance, and lowered fuel consumption[12]. Nanotechnology employs nanoparticles to detect and eliminate environmental contaminants, enhancing environmental protection[13]. Nanomaterials have proven to be valuable in treating wastewater, effectively addressing concerns such as the presence of organic dyes, nitrates, cations, heavy metals, natural organic matter, and viruses.[14]. Sub-100 nm nanoparticles display diverse benefits including improved solar cell absorption, stronger polymer composites, tunable properties, and versatile industrial applications[14]. Zinc oxide nanoparticles serve multiple purposes such as blocking UV rays, acting as antimicrobial agents, functioning as sensors, and improving the capabilities of food packaging[15]. Titanium dioxide nanoparticles exhibit properties that enable self-cleaning, photocatalysis, cosmetic enhancement, and water purification uses, exhibiting size-dependent properties among four material types[16]. Various carbon-based nanomaterials like nanotubes, fullerenes, graphene, and nanofibers are produced using techniques methods like arc discharge, chemical vapor deposition, and laser ablation.[17]. Exceptional carbon-based nanomaterials exhibit widespread industrial utility owing to their remarkable mechanical, optical, electrical, and thermal properties[18]. Inorganic nanomaterials encompass metal, metal oxide, and semiconductor nanoparticles[19]. Developing new synthetic pathways using diverse solvents is vital for creating unique inorganic nanomaterials with applications beyond traditional options, while considering advantages and limitations[20]. Organic nanoparticles, 10 nm to 1 μm in size, comprising polymers and lipids, hold substantial high-tech application value, though often overshadowed by inorganic counterparts like gold and quantum dots[21]. Organic and inorganic nanomaterials undergo noncovalent interactions to achieve desired structures such as micelles, polymers, dendrimers, and liposomal nanoparticles[22]. Composite nanomaterials are intricate multiphase nanoparticles that merge diverse materials for versatile applications[23]. Precisely engineered composite nanomaterials exhibit immense technological potential as sensors, film modifiers, semiconductor-metal junctions, and catalysts, capitalizing on their unique nanoscale properties[24]. Synthetic nanoparticle manufacturing employs chemical, physical, and biological methods with chemical reduction utilizing agents like NaBH4, N2H4, H2 gas, B2H6 gas, and alcohols for cost-effective metal salt reduction[25]. Stabilizing agents regulate nanoparticle features based on their organic, inorganic, or biomolecular nature, encompassing morphology, aggregation, and properties[26]. The solvothermal method includes dissolving precursor metals in a solvent inside an enclosed system, then exposing them to elevated temperature and pressure conditions [27]. Hydrothermal single crystal growth utilizes a pressurized autoclave with hot water and a nutrient to dissolve minerals at high pressure, enabling crystal growth on the cooler side[28]. Hydrothermal synthesis utilizes water as a solvent to create nanomaterials, with reaction conditions and starting material characteristics influencing the resulting properties[29]. The Sol-Gel process combines liquid precursors, hydrolysis, polycondensation, and gel formation to produce transparent sols, which transform into gel networks and yield nanoparticles upon thermal treatment[30]. Co-precipitation is a widely used method for synthesizing metal oxide nanoparticles, with reagent concentration, pH, and heating influencing particle characteristics[30]. Treatment of homogeneous solutions of raw material chlorides/nitrates in solvents with NaOH/NH4OH base results in precipitates that, after salt washing and heating, lead to the production process of metal oxide nanoparticles. [27]. The micro emulsion method involves water and oil phases separated by a surfactant to create nanoemulsions with controlled droplet sizes through precise oil/surfactant ratio adjustment via room temperature stirring[31]. CVD is a versatile technique involving gaseous reactants undergoing surface reactions on a substrate, resulting in solid deposits through heterogeneous reactions, while eliminating by-products via diffusion[32]. The melt mixing method utilizes elevated temperature and shear stress to uniformly disperse metal nanoparticles in a polymer matrix above its Tg, creating thermoplastic polymer-based nanocomposites[33]. High-energy ball milling involves ball collisions in a mill to generate energy for synthesizing oxide nanoparticles, particularly in difficult materials like

nickel-based superalloys[34]. Biosynthesis utilizes viruses, bacteria, plant extracts, and fungi for eco-friendly nanoparticle preparation, differing from toxic chemical methods[35]. Efficiently produces eco-friendly nanoparticles at scale with precise attributes, minimizing pollution[36]. Green chemistry-based nanomaterial synthesis employs safe capping agents, eco-friendly solvents, and eliminates hazardous reducing agents for sustainable and safe production[37]. Plant extract-enabled nanoparticle preparation: a single-step, rapid, safe, and cost-effective synthesis utilizing diverse plant metabolites as reductants and stabilizers[38]. Algae and fruit waste can synthesize metal nanoparticles using algal biomolecules as capping agents, yet toxicity concerns arise, while fruit waste allows direct metal oxide nanoparticle preparation[39]. Nanocomposites feature nano-sized particles for enhanced reinforcement and dispersion within the matrix compared to conventional composites[40]. Nanocomposites synergize continuous matrices and discontinuous reinforcements for heightened optical, mechanical, and thermal conductivities[41]. Natural nanocomposites combine polymers with other components in structures like bones and shells, while synthetic polymer nanocomposites exhibit inferior strength and modulus compared to metal and ceramic counterparts[42]. Polymer nanocomposites optimize mechanical properties through diverse nanoparticles, compositions, flexibility, temperature modulation, and eco-friendly strength, ideal for car parts[43]. Nanoscale Bi-based photocatalysts show potential for water and air toxin removal via visible-light activation, demanding optimization in electron-hole utilization through morphology, heterojunctions, and surface modifications; TiO2 is a well-explored benchmark[44]. Bi nanomaterials serve as photocatalysts due to their appropriate energy band structure, chemical stability, and eco-friendliness[45]. Bi exhibits significant metallic properties due to its lower effective mass, higher Fermi surface, and semiconductor transition ability[46]. Bismuth oxide (Bi2O3) when combined with TiO2 in composites exhibits enhanced visible-light photocatalytic efficiency compared to individual use, finding application in various fields[47]. Bi_2O_3 demonstrates p-type semiconductor characteristics, the valence band edges are positioned around +0.131, while the conduction band edges are situated at approximately +0.334[48]. Bi_2O_3 demonstrates p-type semiconductor characteristics, Identify the locations of the valence band and conduction band edges situated around +0.131 and +0.334 (relative to the normal hydrogen electrode), respectively[49]. Composite materials of Bi-TiO_2 nanotubes were created through both Dual-phase and single-phase anodization techniques, employing different parameters. These composite materials were created with the intention of addressing the treatment needs of industrial wastewater. The evaluation encompassed their effectiveness in visible-light photocatalysis as well as their potential for reuse.

MATERIALS AND METHODS

Chemicals:

Zinc Sulphide, Iodine Crystals (Extra Pure), Tin foil (Extra Pure), Bismuth (Extra Pure), Platinum(Extra Pure), Ethylene glycol, Ethanol (MERCK and SIGMA ALDIRICH), Acetone (MERCK and SIGMA ALDIRICH), Ammonium Flouride (MERCK and SIGMA ALDIRICH).Industrial wastewater; Collected from a Textile industry in Lahore MB; Collected from a company in Lahore.

Method of Sample collection:

A sample of industrial wastewater was collected from a textile facility in Lahore, characterized by its brownish hue. The wastewater from the textile industry in this area contains various pollutants such as dyes and COD (Chemical Oxygen Demand).

Chemicals Concentration Preparation:

A sheet of aluminum foil measuring 5 x 5 cm^2 and with a thickness of 0.2 mm was acquired from MERCK & SIGMA ALDRICH in Karachi, Pakistan. The aluminum foil was of 99.8% purity. Additionally, Ammonium Fluoride (NH_4F) with a purity of 97.0% was obtained from the same source in Karachi, Pakistan.

Synthesis of catalyst:

I created a catalyst using electrochemical anodization through both one-step and two-step methods.

Create a two-stage process for synthesizing Bi-TNT

Initially, I synthesized the Trinitro Toluene catalyst by utilizing a process involving deionized water, ethanol, and acetone. To eliminate impurities, I subjected tin foil to sonication. The electrolytic solution was prepared using 1 wt% NH_4F, 5 wt% deionized water, and 94 wt% ethylene glycol. Employing an N6702A Agilent Technologies power supply, I conducted electrochemical anodization at 50 volts over 2 hours, with platinum (Pt) serving as the cathode and tin foil as the anode. Subsequently, the anodized tin foil underwent washing with distilled water and ethyl alcohol, followed by drying under nitrogen gas. The tin foil underwent a process of annealing in a furnace at 550°C for duration of 1.5 hours. This procedure led to the achievement of the intended crystalline configuration of tin oxide (TiO2). In a separate step, I introduced bismuth to the anodized Trinitro Toluene using an electrochemical deposition technique. Platinum was employed as the cathode, and the anodized Trinitro Toluene acted as the anode. Varying concentrations of bismuth electrolyte solutions, ranging from 2.0 wt% to 0.5 wt%, were prepared and utilized. Through trials involving different bismuth deposition times (one to fifteen minutes) and voltages (ranging from 40 to 70 volts), successful electrochemical deposition of bismuth onto the Trinitro Toluene was achieved. After being deposited, the specimens underwent a purification process using distilled water, followed by drying in a digital oven at 70°C for a period of 10 hours.

Single-step production of Bi-TNT through synthesis

Bismuth trinitrotoluene was created for the purpose of eliminating impurities. Tin foils were cleaned using distilled water, ethyl alcohol, and acetone for ten minutes. An electrolytic solution consisting of 5 wt% distilled water, 1 wt% NH4F, and ethylene glycol was used in combination with varying bismuth concentrations (ranging from 2 wt% to 0.5 wt %) and voltage levels (from 30 volts to 60 volts). Electrochemical anodization was carried out for durations of one to four hours, using the necessary materials. Following anodization, the tin foils were washed with distilled water and dried using nitrogen gas. Subsequently, the tin foils were annealed at 550 ℃ in a furnace for 1.5 hours to enhance their crystalline structure and overall characteristics.

Photocatalytic experiment:

Composite efficiency in photodegradation was achieved in two steps. The initial part involved optimizing the photodegradation conditions for Bismuth tri nitro Toluene (Bi-TNT) alongside the degradation of Methylene Blue (MB). In the latter part, the optimized conditions were applied to industrially generated waste for photodegradation. The experimental arrangement consisted of a photocatalytic reactor, as described in the Supplementary Materials section. The procedure involved a 35 mL solution with an initial concentration of 5 mg L^{-1} of MB. A visible-light source, specifically a Philips fluorescent lamp that emitted light with an intensity of 31 W m^{-2} and wavelengths spanning from 400 nm to 700 nm, was employed to facilitate the photocatalytic reactions. Prior to initiating the photocatalytic tests, the catalysts were allowed to establish adsorption equilibrium in the absence of light for 25 minutes. The reduction of MB was quantified at 665 nm using a UV–Vis spectrometer. The source of the industrial wastewater was the Lahore Industrial Complex in the Republic of Pakistan, originating from the textile industry's dyeing and coloring processes. The wastewater potentially contains pollutants such as Trichloroethylene, Formaldehyde, Chromium, Nickel, Lead, Hydrochloric Acid, Phenol, and dyes[50]. The conditions for photodegradation of wastewater of industry were similar as related to the Methylene blue photodegradation test. A Shimadzu TOC-L CPH instrument from Japan was employed to analyze the total organic carbon (TOC) content in industrial wastewater. A durability assessment was performed on both one-step and two-step Bi-TNT catalysts to gauge their photodegradation stability. This test aimed to determine the long-term performance of the photocatalysts under conditions identical to those utilized for assessing the photodegradation efficiency of MB dye and industrial wastewater, aimed at refining the recycling process. The Bi-TNT catalysts underwent five rounds of rinsing with distilled water, with each round lasting

ten minutes. Subsequently, they were dried in an oven at sixty degrees Celsius for thirty minutes to ensure the removal of any impurities adhering to the Bi-TNT surface. COD = chemical oxygen demand, SS = suspended solids.

Sr.no	Parameter	Unit	Value
1	TOC	mgL^{-1}	55
2	COD	mgL^{-1}	290
3	pH	-	7.20
4	SS	mgL^{-1}	80
5	Temperature	℃	32

Table 1.1 Attributes of industrial wastewater.

Results and Discussion

FE-SEM

The diagram provided illustrates the structural differences between one-step and two-step Bi-TNT composites, along with pure TNT, as observed through FE-SEM imaging. The fabrication process effectively resulted in tin oxide (TiO2) nanotubes on a tin foil substrate. These nanotubes displayed lengths ranging from 1800 to 2100 nm and diameters of 50-60 nm, as shown in Figure 1.1. The configuration of TiO2 nanotubes was consistent, displaying exposed ends and distinct gaps between individual tubes. For the experiment concerning photocatalytic degradation, optimal circumstances were determined for both the two-step and one-step synthesis methods of Bi-TNTs. In the two-step approach, the most favorable results were achieved when utilizing 1.0 wt% bismuth (Bi) concentration. This concentration was obtained by applying a Bi layer onto the surface for duration of 5 minutes at 60 V, as shown in Figure 1(b). Conversely, employing the one-step Bi-TNT method demonstrated its best performance with a Bi concentration of 1.5 wt%. This entailed anodization over a period of 2 hours at 50 V, as depicted in Figure 1(c). The FE-SEM images displayed successful incorporation of Bi onto the TiO2 surface using both synthesis methods, while retaining the characteristic nanotube morphology even after the Bi deposition process.

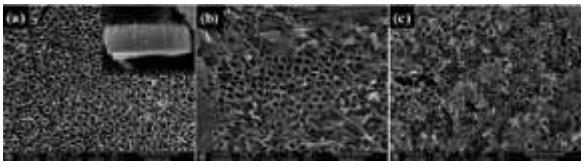

1.1 Micrographs obtained via Field Emission Electron Scanning Microscopy (FEE-SEM) depict the structures of (a) TNT and Bi-TNT, (b) composites created through a two-step process, and (c) composites synthesized using a one-step method.

XRD

XRD analyses demonstrated that the TNT and Bi-TNT catalysts, synthesized through both two-step and one-step procedures, yielded similar patterns, exhibited a crystalline structure of anatase phase after being annealed at 550 °C for 1.5 hours, as depicted in Figure 2(a). The XRD data also indicated the presence of both titanium (Ti) and bismuth (Bi) peaks. The bismuth existed in a distinct Bi2O3 phase. The diffraction peaks corresponding to the anatase phase of titanium dioxide (TiO2) were detected at specific angles, namely 25.1°, 38.1°, 48.5°, and 78.0°[51]. The diffraction signals occurring at angles of 37.3° and 55.8° in the 2θ range were identified as characteristic peaks corresponding to bismuth (Bi) material[52].

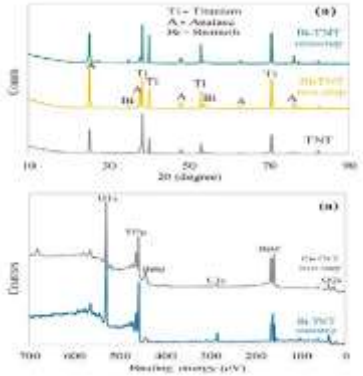

Fig. 1.2: Bi-TNT composites: (a) XRD spectra and (b) XPS spectra of the complete range.

UV–Vis diffuses reflectance spectra

Figure 1.3 illustrates the UV-Vis diffuse reflectance spectra (UV-Vis DRS) were recorded for composite materials comprising TNT and Bi-TNT. These composites were fabricated using both single-step and two-step methods. The band-gap energies were determined through the utilization of the Tauc plot technique coupled with the Kubelka-Munk function. In the ultraviolet (UV) range, the TNT composite

demonstrated notable absorption characteristics, indicative of band-gap energy of approximately 3.21 eV. Conversely, both the one-step and two-step synthesized Bi-TNT catalysts exhibited absorbance within the visible spectrum, revealing energy band-gaps of approximately 2.87 and 2.81, respectively. It is worth noting that significant absorption peaks were identified in the TNT absorption spectrum, occurring at approximately 435 nm and 650 nm, corresponding to h+ and e- absorption, as reported in earlier research. Importantly, the incorporation of bismuth (Bi) in the Bi-TNT composites led to a more prominent absorption in the visible region compared to the pure TNT composite.

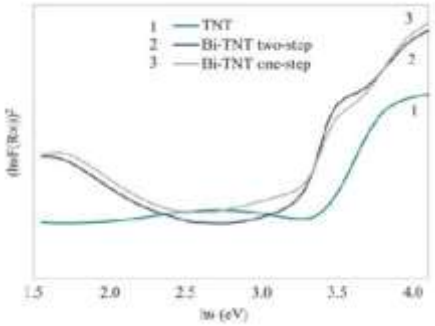

Fig.1.3: UV-Vis diffuse reflectance spectroscopy (UV-Vis DRS) was employed to analyze the Tauc plot of both TNT and Bi-TNT catalysts, considering both one-step and two-step processes.

Treating industrial wastewater with improved outcomes derived from optimization

The efficiency of using Bi-TNT catalysts to treat industrial wastewater was investigated through both one-step and two-step synthesis approaches. The most advantageous settings for creating the two-step Bi-TNT catalyst involved using a Bi concentration of 1.0 wt% and applying a 5-minute Bi deposition at 60 V. In comparison, for the single-step Bi-TNT synthesis, the best results were achieved by utilizing a Bi concentration of 1.5 wt% and performing anodization for 2 hours at 50 V. When compared to the conventional TNT catalyst, both Bi-TNT catalysts displayed superior photodegradation performance under visible light for 6-hour duration. The extended treatment time was necessary due to the complex mixture of dyes and chemicals present in industrial wastewater, requiring more degradation time than simpler compounds like MB. The initial concentration of total organic carbon (TOC) in the wastewater was 45 mg L−1. After applying photocatalytic treatment, the TOC levels were lowered to 34 mg L−1, 24 mg L−1, and 19 mg L−1, using TNT, and two-step Bi-TNT, and one-step Bi-TNT catalysts respectively. These reductions in TOC translate to percentage decreases of 22%, 44%, and 56% for TNT, two-step Bi-TNT, and one-step Bi-TNT respectively. Notably, the two-step and one-step Bi-TNT composites exhibited TOC removal rates that were 2.0 and 2.5 times higher compared to TNT.

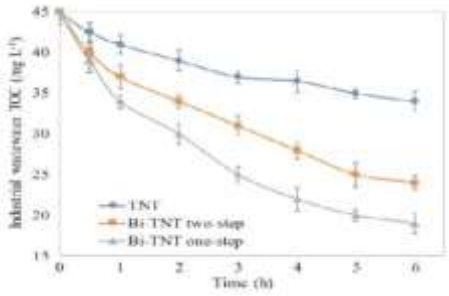

Fig. 1.4: Efficient photocatalysts made of TNT, as well as both one-step and two-step Bi-TNT composites, have demonstrated promising outcomes in the treatment of industrial wastewater.

Alterations to TiO2 with bismuth (Bi) for enhancing photocatalytic mechanisms

The Supplementary materials Fig. S5 illustrates a proposed photocatalytic mechanism for Bi-TNT. This process involves several steps: To begin, the surface of Bi-deposited TiO2 becomes responsive to visible light. As a result, when electrons generated by light exposure move from the valence band (VB) of TiO2 to its conduction band (CB), this triggers the formation of holes (h+) in the valence band of Bi. These newly formed electrons and holes then initiate a reaction with water (H2O), resulting in the creation of hydroxyl (OH) radicals and superoxide ions. Operating in coordination, these electrons, vacancies in the valence band, hydroxyl radicals, and superoxide ions cooperate to achieve their collective goal break down and degrade pollutants.[53]. In the process of photocatalytic degradation, the initial step involves the conversion of MB into intermediate

substances, which subsequently undergo further degradation into CO2 and H2O. The presence of bismuth (Bi) has a beneficial impact on the efficiency of TiO2 in this degradation process under visible-light conditions. This improvement stems from Bi's ability to enhance the utilization of photons from visible light for the generation of electron-hole pairs (e- and h+). Moreover, the presence of Bi on the surface of TiO2 promotes the effective separation of these photoexcited electron-hole pairs, leading to an increased production of superoxides and OH radicals[54]. The enhanced efficiency of Bi deposition in photodegradation could arise from multiple reasons: Incorporating Bi through deposition could reduce the energy band gap, leading to an enhancement in TiO_2 light absorption in the visible range. When Bi is added to the surface of TiO2, it has the ability to trap excited electrons, which in turn lessens the recombination of electron-hole pairs. This leads to an enhancement in the creation of superoxides and OH radicals. Furthermore, the increased surface area of the Bi-TNT combination offers a greater capability for trapping pollutants. This results in the formation of more sites that exhibit catalytic activity[55].

Reference

1. He, R., et al., *Review on nanoscale Bi-based photocatalysts.* Nanoscale Horizons, 2018. **3**(5): p. 464-504.
2. Gallo, J.C., J.L. Craycraft, and S.C. Bush, *Guess who came to dinner: An empirical study of federal antitrust enforcement for the period 1963–1984.* Review of Industrial Organization, 1985. **2**: p. 106-130.
3. Barad, K.H., D. Sharma, and V. Vyas, *Crack detection in cantilever beam by frequency based method.* procedia engineering, 2013. **51**: p. 770-775.
4. Vedam, S., et al., *Acquiring a four-dimensional computed tomography dataset using an external respiratory signal.* Physics in Medicine & Biology, 2002. **48**(1): p. 45.
5. Gallo, C., B. Chandrasekhar, and P. Sutter, *Transport properties of bismuth single crystals.* Journal of Applied Physics, 1963. **34**(1): p. 144-152.
6. ARICAK, F. and E. ÇAĞLARER, *NANOTEKNOLOJİK GELİŞMELERDE İŞ SAĞLIĞI VE GÜVENLİĞİ.* SOSYAL BEŞERİ VE İDARİ BİLİMLER ALANINDA ULUSLARARASI ARAŞTIRMALAR X, 2023: p. 157.
7. Tripathi, A., et al., *The gut–liver axis and the intersection with the microbiome.* Nature reviews Gastroenterology & hepatology, 2018. **15**(7): p. 397-411.
8. Klimont, Z., et al., *Global anthropogenic emissions of particulate matter including black carbon.* Atmospheric Chemistry and Physics, 2017. **17**(14): p. 8681-8723.
9. Puzanov, I., et al., *Managing toxicities associated with immune checkpoint inhibitors: consensus recommendations from the Society for Immunotherapy of Cancer (SITC) Toxicity Management Working Group.* Journal for immunotherapy of cancer, 2017. **5**(1): p. 1-28.
10. Salata, O.V., *Applications of nanoparticles in biology and medicine.* Journal of nanobiotechnology, 2004. **2**(1): p. 1-6.
11. Bhattacharya, P. and A.F. Keating, *Impact of environmental exposures on ovarian function and role of xenobiotic metabolism during ovotoxicity.* Toxicology and applied pharmacology, 2012. **261**(3): p. 227-235.
12. Yan, L., C. Rong, and G. Zhao. *Strengthen cloud computing security with federal identity management using hierarchical identity-based cryptography*. in *Cloud Computing: First International Conference, CloudCom 2009, Beijing, China, December 1-4, 2009. Proceedings 1*. 2009. Springer.
13. Karn, B., T. Kuiken, and M. Otto, *Nanotechnology and in situ remediation: a review of the benefits and potential risks.* Environmental

health perspectives, 2009. **117**(12): p. 1813-1831.
14. Amin, T. and M. Thakur, *A comparative study on proximate composition, phytochemical screening, antioxidant and antimicrobial activities of Linum usitatisimum L.(flaxseeds).* International Journal of Current Microbiology and Applied Sciences, 2014. **3**(4): p. 465-481.
15. Sruthi, T., et al., *Stabilized landfill leachate treatment using heterogeneous Fenton and electro-Fenton processes.* Chemosphere, 2018. **210**: p. 38-43.
16. Buzea, C., I.I. Pacheco, and K. Robbie, *Nanomaterials and nanoparticles: sources and toxicity.* Biointerphases, 2007. **2**(4): p. MR17-MR71.
17. Gilkerson, T., *Understanding Carbon Nanoparticle Transport in Saturated Porous Media: The Influence of Dissolved Organic Matter*. 2020, Colorado State University.
18. Wei Seh, Z., et al., *Sulphur–TiO2 yolk–shell nanoarchitecture with internal void space for long-cycle lithium–sulphur batteries.* Nature communications, 2013. **4**(1): p. 1331.
19. Ferrando, R., J. Jellinek, and R.L. Johnston, *Nanoalloys: from theory to applications of alloy clusters and nanoparticles.* Chemical reviews, 2008. **108**(3): p. 845-910.
20. Li, S., et al., *Water quality in relation to land use and land cover in the upper Han River Basin, China.* Catena, 2008. **75**(2): p. 216-222.
21. Uddin, M. and A.R. Chowdhury. *Integration of nanotechnology into the undergraduate engineering curriculum*. in *International Conference on Engineering Education*. 2001. Citeseer.
22. Jeevanandam, J., et al., *Review on nanoparticles and nanostructured materials: history, sources, toxicity and regulations.* Beilstein journal of nanotechnology, 2018. **9**(1): p. 1050-1074.
23. Calandra, M., *Chemically exfoliated single-layer MoS 2: Stability, lattice dynamics, and catalytic adsorption from first principles.* Physical Review B, 2013. **88**(24): p. 245428.
24. Della Porta, G. and E. Reverchon, *Modular Tissue Engineering: An Artificial Extracellular Matrix to Address and Stimulate Regeneration/Differentiation.* Extracellular Matrix for Tissue Engineering and Biomaterials, 2018: p. 191-210.
25. Lenzini, F., et al., *Integrated photonic platform for quantum information with continuous variables.* Science advances, 2018. **4**(12): p. eaat9331.
26. Burtness, B., et al., *Pembrolizumab alone or with chemotherapy versus cetuximab with chemotherapy for recurrent or metastatic squamous cell carcinoma of the head and neck (KEYNOTE-048): a randomised, open-label, phase 3 study.* The Lancet, 2019. **394**(10212): p. 1915-1928.
27. Soytas, M.A., M. Denizel, and D.D. Usar, *Addressing endogeneity in the causal relationship between sustainability and financial performance.* International Journal of Production Economics, 2019. **210**: p. 56-71.
28. Rane, A.V., et al., *Methods for synthesis of nanoparticles and fabrication of nanocomposites*, in *Synthesis of inorganic nanomaterials*. 2018, Elsevier. p. 121-139.
29. Stankic, S., et al., *Pure and multi metal oxide nanoparticles: synthesis, antibacterial and cytotoxic properties.* Journal of nanobiotechnology, 2016. **14**(1): p. 1-20.
30. Wijayawardene, N.N., et al., *Notes for genera: Ascomycota.* Fungal diversity, 2017. **86**: p. 1-594.
31. Anton, N. and T.F. Vandamme, *Nano-emulsions and micro-emulsions:*

clarifications of the critical differences. Pharmaceutical research, 2011. **28**: p. 978-985.
32. Alonso, J.M., et al., *Genome-wide insertional mutagenesis of Arabidopsis thaliana.* Science, 2003. **301**(5633): p. 653-657.
33. Pramanik, S.K., et al., *The anaerobic digestion process of biogas production from food waste: Prospects and constraints.* Bioresource Technology Reports, 2019. **8**: p. 100310.
34. Rane, A. and A. Kumar. *Sentiment classification system of twitter data for US airline service analysis*. in *2018 IEEE 42nd Annual Computer Software and Applications Conference (COMPSAC)*. 2018. IEEE.
35. Jose, J.V., A.M. Ealias, and M. Saravanakumar, *Carbon Encapsulated Zero-Valent Iron Nanoparticle Using Abelmoschus esculentus (Lady's Finger) Extract as an Adsorbent for Cr (VI) in Aqueous Solution.* Nature Environment & Pollution Technology, 2017. **16**(1).
36. Mittal, A.K., Y. Chisti, and U.C. Banerjee, *Synthesis of metallic nanoparticles using plant extracts.* Biotechnology advances, 2013. **31**(2): p. 346-356.
37. Zhou, H., et al., *Interface engineering of highly efficient perovskite solar cells.* Science, 2014. **345**(6196): p. 542-546.
38. Makarov, V., et al., *"Green" nanotechnologies: synthesis of metal nanoparticles using plants.* Acta Naturae (англоязычная версия), 2014. **6**(1 (20)): p. 35-44.
39. O'Reilly, C.M., et al., *Rapid and highly variable warming of lake surface waters around the globe.* Geophysical Research Letters, 2015. **42**(24): p. 10,773-10,781.
40. Mansbridge, N., et al., *Feature selection and comparison of machine learning algorithms in classification of grazing and rumination behaviour in sheep.* Sensors, 2018. **18**(10): p. 3532.
41. Elbaz, D., et al., *GOODS–Herschel: an infrared main sequence for star-forming galaxies.* Astronomy & Astrophysics, 2011. **533**: p. A119.
42. Coad, B.W. and N.A. Hussain, *First record of the exotic species Hemiculter leucisculus (Actinopterygii: Cyprinidae) in Iraq.* Zoology in the Middle East, 2007. **40**(1): p. 107-109.
43. Khan, M., et al., *Optimization of process parameters for production of volatile fatty acid, biohydrogen and methane from anaerobic digestion.* Bioresource technology, 2016. **219**: p. 738-748.
44. Iazdani, F. and A. Nezamzadeh-Ejhieh, *The photocatalytic rate of ZnO supported onto natural zeolite nanoparticles in the photodegradation of an aromatic amine.* Environmental Science and Pollution Research, 2021. **28**(38): p. 53314-53327.
45. Ji, D., et al., *Prevalence of psychological symptoms among Ebola survivors and healthcare workers during the 2014-2015 Ebola outbreak in Sierra Leone: a cross-sectional study.* Oncotarget, 2017. **8**(8): p. 12784.
46. Matilla, A., et al. *Three-dimensional measurements with a novel technique combination of confocal and focus variation with a simultaneous scan*. in *Optical Micro-and Nanometrology VI*. 2016. SPIE.
47. Wu, J., et al., *Ang-(1–7) exerts protective role in blood–brain barrier damage by the balance of TIMP-1/MMP-9.* European journal of pharmacology, 2015. **748**: p. 30-36.
48. Cole, J.R., et al., *The Ribosomal Database Project: improved alignments and new tools for rRNA analysis.* Nucleic acids research, 2009. **37**(suppl_1): p. D141-D145.
49. Yang, J., et al., *Continuous nonsingular terminal sliding mode control for systems with mismatched disturbances.* Automatica, 2013. **49**(7): p. 2287-2291.
50. Chow, P.K., et al., *SIRveNIB: selective internal radiation therapy versus sorafenib in Asia-Pacific patients with*

hepatocellular carcinoma. Journal of clinical oncology, 2018. **36**(19): p. 1913-1921.

51. Hudari, F.F., et al., *Voltammetric sensor for simultaneous determination of p-phenylenediamine and resorcinol in permanent hair dyeing and tap water by composite carbon nanotubes/chitosan modified electrode.* Microchemical Journal, 2014. **116**: p. 261-268.
52. Yuan, H.-S., et al., *Fungal diversity notes 1277–1386: taxonomic and phylogenetic contributions to fungal taxa.* Fungal Diversity, 2020. **104**: p. 1-266.
53. Marino, M., et al., *Measuring sleep: accuracy, sensitivity, and specificity of wrist actigraphy compared to polysomnography.* Sleep, 2013. **36**(11): p. 1747-1755.
54. Xu, H., et al., *Information privacy concerns: Linking individual perceptions with institutional privacy assurances.* Journal of the Association for Information Systems, 2011. **12**(12): p. 1.
55. Li, X., et al., *Antimicrobial activities of ZnO powder-coated PVC film to inactivate food pathogens.* International journal of food science & technology, 2009. **44**(11): p. 2161-2168.